

---

## Studying the Vibrational Behavior of Single-Walled Carbon Nanotubes under Different Boundary Conditions using the Rayleigh-Ritz Technique

R. Ansari<sup>1</sup>, H. Rouhi, S. Sahmani

*Department of Mechanical Engineering, University of Guilan, P.O. Box 3756, Rasht, Iran*

<sup>1</sup>*Corresponding author: r\_ansari@guilan.ac.ir*

*Received date: July 2016  
Accepted date: August 2016*

### **Abstract**

*The vibrational response of single-walled carbon nanotubes (SWCNTs) is studied in this paper. To take size effects into account, Eringen's nonlocal elasticity equations are incorporated into the Donnell shell theory. The Rayleigh-Ritz method is employed in conjunction with the polynomial series as modal displacement functions to solve the problem. Four commonly used boundary conditions namely as simply supported-simply supported, clamped-clamped, clamped-simply supported, and clamped-free are considered. The fundamental frequencies of SWCNTs with various values of aspect ratios and nonlocal parameters are obtained. To propose the proper values of nonlocal parameter, the results of nonlocal shell model are matched with those of molecular dynamics (MD) simulations for armchair and zigzag SWCNTs through a nonlinear least square fitting procedure. The appropriate values of nonlocal parameter corresponding to each type of chirality and boundary condition are then derived. It is found that the results obtained via the presented nonlocal shell model with its proposed proper values of nonlocal parameter are in excellent agreement with those of MD simulations.*

**Keywords:** Carbon nanotube; Nonlocal elasticity; Free vibration; Donnell shell theory; Molecular dynamics simulation

## **1. Introduction**

After the discovery of carbon nanotubes (CNTs) by Iijima [1], the applications of these attractive nanostructures have been increasing in recent years due to their outstanding physical, mechanical, and electrical properties. They have provided new building block in various emerging fields of nanoscience and nanotechnology [2-7].

As the results predicted by the classical continuum models are independent of the influence of small scale of nanostructures, they become controversial to implement for the analyses of such nanoscale systems. Hence, the extension of the continuum mechanics to accommodate the size dependence of nanostructures becomes a topic of major concern. To incorporate the size effects that exist at nanoscale into the classical continuum theory, it is needed to refine the classical model. Modified continuum models are widely applied in nanomechanics due to their computational efficiency and the capability to produce accurate results which are comparable to those of atomistic models. The use of nonlocal elasticity for nanostructures was applied for the first time by Peddieson et al. [8]. After that, nonlocal continuum model has gained much popularity among the researchers because of its efficiency as well as simplicity to analyze the behavior of various nanostructures.

Ghorbanpour-Arani and Zarei [9] studied surface and small scale effects on free transverse vibration of a single-walled carbon nanotube with Y-junction at downstream end conveying viscose fluid based on the nonlocal Euler-Bernoulli beam theory. Hu et al. [10] investigated the transverse and torsional wave in SWCNT and DWCNT using nonlocal single and double elastic cylindrical shells. They found that the van der Waals interaction has little effect on the phase difference of transverse wave. Niknam and Aghdam [11] obtained a closed form solution for both natural frequency and buckling load of nonlocal functionally graded beams resting on nonlinear elastic foundation. Adhikari et al. [12] introduced the idea of nonlocal normal modes arising in the dynamic analysis of nanoscale structures. Ansari et al. [13] also developed a nonlocal finite element model which accounts for the small scale effects on free vibration of multi-layered graphene sheets. There are so many other research works in which the behaviors of nanostructures under various loading conditions have been predicted based on nonlocal elasticity continuum models [14-25].

The Rayleigh-Ritz technique is one of the well qualified numerical methods which has been employed in many studies. An investigation of the literature shows that there are many works in which the Rayleigh-Ritz technique has been applied to predict the vibrational behavior of various structures. Zhou [26] applied Rayleigh-Ritz method using a set of Timoshenko beam

functions to analyze the free vibration of Mindlin rectangular plates with uniform edge constraints. Al-Obeid and Cooper [27] developed the Rayleigh-Ritz method using polynomial functions to study the vibration properties of composite laminates plates.

Continuing with the vibration problems, Roufaeil and Dawe [28] investigated the flexural vibration of isotropic rectangular plates including the presence of membrane stress system based on Rayleigh-Ritz technique of analysis. Recently, Lee and his coworkers [29] analyzed the effect of thermal vibration on the resonant frequency of transverse vibration of scanning thermal microscope using the Rayleigh-Ritz technique to solve the vibration problem of the probe nanomachining.

In the present work, the Rayleigh-Ritz technique is employed to predict the vibrational response of SWCNTs with four common sets of boundary conditions. The components of displacement are represented as functions of polynomial series to implement the Rayleigh-Ritz method to the governing equations of nonlocal shell model. To obtain the appropriate values of nonlocal parameter corresponding to each boundary condition, MD simulations results for various SWCNTs are matched with those of nonlocal continuum model. To this end, a nonlinear least square fitting procedure is established in which the nonlocal parameter is set as the optimization variable. It is observed that the present nonlocal shell model with its proper values of nonlocal parameter has the capability to predict the free vibration behavior of SWCNTs with an excellent accuracy which is comparable with the results of MD simulation.

## 2. The Nonlocal Elastic Shell Model for CNTs

### 2.1. Donnell Shell Equations based on Nonlocal Elasticity

The theory of nonlocal elasticity was first considered by Eringen [30]. In the nonlocal model, in contrast to the classical elasticity, the stress at a reference point  $x$  in an elastic body depends not only on the strains at  $x$ , but also on strains at all other points of the body [30]. The nonlocal constitutive equation is given by [31]

$$(1 - \mu \nabla^2) \boldsymbol{\sigma} = \mathbf{t} \quad (1)$$

where  $\mu$  is the nonlocal parameter used in nonlocal continuum;  $\mathbf{t}$  is the macroscopic stress tensor at a point. In the limit when the characteristic length goes to zero, the nonlocal elasticity reduces to the local elasticity. The stress tensor is related to strain by generalized Hooke's law as

$$\mathbf{t} = \mathbf{S} : \boldsymbol{\epsilon} \quad (2)$$

here  $\mathbf{S}$  is the fourth-order elasticity tensor and ‘ $\cdot$ ’ denotes the double dot product. Hooke’s law for the stress and strain relation is thus expressed by

$$\begin{Bmatrix} \sigma_x \\ \sigma_y \\ \sigma_{xy} \\ \sigma_{yz} \\ \sigma_{xz} \end{Bmatrix} - \mu \nabla^2 \begin{Bmatrix} \sigma_x \\ \sigma_y \\ \sigma_{xy} \\ \sigma_{yz} \\ \sigma_{xz} \end{Bmatrix} = \begin{bmatrix} E & \nu E & 0 & 0 & 0 \\ 1-\nu^2 & 1-\nu^2 & 0 & 0 & 0 \\ \nu E & E & 0 & 0 & 0 \\ 1-\nu^2 & 1-\nu^2 & 0 & 0 & 0 \\ 0 & 0 & 2G & 0 & 0 \\ 0 & 0 & 0 & G & 0 \\ 0 & 0 & 0 & 0 & G \end{bmatrix} \begin{Bmatrix} \varepsilon_{xx} \\ \varepsilon_{yy} \\ \gamma_{xy} \\ \gamma_{yz} \\ \gamma_{xz} \end{Bmatrix} \quad (3)$$

Figure 1 shows the cylindrical shell of length  $L$ , radius  $R$  and thickness  $h$  with its coordinate system  $(r, \theta, x)$  as  $x$ -axis is along the length of the shell.

Based on Donnell shell theory [32], the displacements  $u, v, w$  and the rotations  $\psi_x, \psi_\theta$  can be expressed in the following form

$$u_x(x, \theta, z, t) = u(x, \theta, t) + z\psi_x(x, \theta, t) \quad (4-a)$$

$$u_y(x, \theta, z, t) = v(x, \theta, t) + z\psi_\theta(x, \theta, t) \quad (4-b)$$

$$u_z(x, \theta, z, t) = w(x, \theta, z, t) \quad (4-c)$$

which yields the following kinematics relations for normal strains  $\varepsilon_{xx}$  and  $\varepsilon_{yy}$  and shear strains  $\gamma_{xy}, \gamma_{yz}$ , and  $\gamma_{xz}$  as

$$\begin{aligned} \varepsilon_{xx} &= \frac{\partial u}{\partial x} \quad , \quad \varepsilon_{\theta\theta} = \frac{1}{R} \frac{\partial v}{\partial \theta} + \frac{w}{R} \quad , \\ \gamma_{xy} &= \frac{\partial v}{\partial x} + \frac{1}{R} \frac{\partial u}{\partial \theta} \quad , \quad \gamma_{xz} = \frac{\partial w}{\partial x} + \psi_x \\ \gamma_{\theta z} &= \frac{1}{R} \frac{\partial w}{\partial \theta} - \frac{v}{R} + \psi_\theta \end{aligned} \quad (5)$$

From equations (3-5), the nonlocal force and moment resultants according to the coupled Donnell shell theory become

$$N_{xx} = \int_{-h/2}^{h/2} \sigma_{xx} dz \quad i. e. \quad N_{xx} - \mu \nabla^2 N_{xx} = \frac{Eh}{1-\nu^2} \frac{\partial u}{\partial x} + \frac{\nu Eh}{1-\nu^2} \left( \frac{1}{R} \frac{\partial v}{\partial \theta} + \frac{w}{R} \right) \quad (6-a)$$

$$N_{\theta\theta} = \int_{-h/2}^{h/2} \sigma_{\theta\theta} dz \quad i. e. \quad N_{\theta\theta} - \mu \nabla^2 N_{\theta\theta} = \frac{\nu Eh}{1-\nu^2} \frac{\partial u}{\partial x} + \frac{Eh}{1-\nu^2} \left( \frac{1}{R} \frac{\partial v}{\partial \theta} + \frac{w}{R} \right) \quad (6-b)$$

$$N_{x\theta} = \int_{-h/2}^{h/2} \sigma_{x\theta} dz \quad i. e. \quad N_{x\theta} - \mu \nabla^2 N_{x\theta} = Gh \left( \frac{\partial v}{\partial x} + \frac{1}{R} \frac{\partial u}{\partial \theta} \right)$$

(6-c)

$$M_{xx} = \int_{-h/2}^{h/2} z\sigma_{xx} dz \quad i. e. \quad M_{xx} - \mu\nabla^2 M_{xx} = D \left( \frac{\partial\psi_x}{\partial x} + \frac{\nu}{R} \frac{\partial\psi_\theta}{\partial\theta} \right)$$

(6-d)

$$M_{\theta\theta} = \int_{-h/2}^{h/2} z\sigma_{\theta\theta} dz \quad i. e. \quad M_{\theta\theta} - \mu\nabla^2 M_{\theta\theta} = D \left( \frac{1}{R} \frac{\partial\psi_\theta}{\partial\theta} + \nu \frac{\partial\psi_x}{\partial x} \right)$$

(6-e)

$$M_{x\theta} = \int_{-h/2}^{h/2} z\sigma_{x\theta} dz \quad i. e. \quad M_{x\theta} - \mu\nabla^2 M_{x\theta} = \frac{1}{2} D(1-\nu) \left( \frac{\partial\psi_\theta}{\partial x} + \frac{1}{R} \frac{\partial\psi_x}{\partial\theta} \right)$$

(6-f)

$$Q_{xx} = \int_{-h/2}^{h/2} \sigma_{xz} dz \quad i. e. \quad Q_{xx} - \mu\nabla^2 Q_{xx} = Gh \left( \frac{\partial w}{\partial x} + \psi_x \right)$$

(6-g)

$$Q_{\theta\theta} = \int_{-h/2}^{h/2} \sigma_{\theta z} dz \quad i. e. \quad Q_{\theta\theta} - \mu\nabla^2 Q_{\theta\theta} = Gh \left( \frac{1}{R} \frac{\partial w}{\partial\theta} - \frac{\nu}{R} + \psi_\theta \right)$$

(6-h)

where  $D = 0.85 eV$  denotes the bending rigidity of the shell.

The governing equations on the basis of the Donnell shell theory can be given as [32]

$$\frac{\partial N_{xx}}{\partial x} + \frac{1}{R} \frac{\partial N_{x\theta}}{\partial\theta} = I_1 \ddot{u} + I_2 \ddot{\psi}_x \quad (7-a)$$

$$\frac{\partial N_{x\theta}}{\partial x} + \frac{1}{R} \frac{\partial N_{\theta\theta}}{\partial\theta} + \frac{Q_{\theta\theta}}{R} = I_1 \ddot{v} + I_2 \ddot{\psi}_\theta$$

(7-b)

$$\frac{\partial Q_{xx}}{\partial x} + \frac{1}{R} \frac{\partial Q_{\theta\theta}}{\partial\theta} - \frac{N_{\theta\theta}}{R} = I_1 \ddot{w} \quad (7-c)$$

$$\frac{\partial M_{xx}}{\partial x} + \frac{1}{R} \frac{\partial M_{x\theta}}{\partial\theta} - Q_{xx} = I_2 \ddot{u} + I_3 \ddot{\psi}_x \quad (7-d)$$

$$\frac{\partial M_{x\theta}}{\partial x} + \frac{1}{R} \frac{\partial M_{\theta\theta}}{\partial\theta} - Q_{\theta\theta} = I_2 \ddot{v} + I_3 \ddot{\psi}_\theta \quad (7-e)$$

## 2.2. Field equations for vibrations of SWCNTs

Substituting equations (6) into (7) yields the field equations corresponding to nonlocal Donnell shell model as

$$\frac{Eh}{1-\nu^2} u_{,xx} \pm \frac{1}{2} \left( \frac{1}{R} \right)^2 \frac{Eh}{2(1+\nu)} u_{,\theta\theta} + \frac{1}{R} \left( \frac{\nu Eh}{1-\nu^2} + \frac{1}{2} \frac{Eh}{2(1+\nu)} \right) v_{,x\theta}$$

$$\begin{aligned}
 & + \frac{1}{R} \frac{\nu Eh}{1-\nu^2} w_{,x} = I_1 \ddot{u} + I_2 \ddot{\psi}_x - \\
 & \mu \left[ I_1 \left( \ddot{u}_{,xx} + \frac{1}{R^2} \ddot{u}_{,\theta\theta} \right) + I_2 \left( \ddot{\psi}_{x,xx} + \frac{1}{R^2} \ddot{\psi}_{x,\theta\theta} \right) \right] \\
 & (8-a)
 \end{aligned}$$

$$\begin{aligned}
 & \frac{1}{R} \left( \frac{\nu Eh}{1-\nu^2} + \frac{1}{2} \frac{Eh}{2(1+\nu)} \right) u_{,x\theta} + \frac{1}{2} \frac{Eh}{2(1+\nu)} v_{,xx} - \\
 & \left( \frac{1}{R} \right)^2 \frac{Eh}{1-\nu^2} v_{,\theta\theta} - \frac{Gh}{R^2} v - \left( \frac{1}{R} \right)^2 \left( \frac{Eh}{1-\nu^2} + Gh \right) w_{,\theta} + \\
 & \frac{Gh}{R} \psi_{\theta} = I_1 \ddot{v} + I_2 \ddot{\psi}_{\theta} - \\
 & \mu \left[ I_1 \left( \ddot{v}_{,xx} + \frac{1}{R^2} \ddot{v}_{,\theta\theta} \right) + I_2 \left( \ddot{\psi}_{\theta,xx} + \frac{1}{R^2} \ddot{\psi}_{\theta,\theta\theta} \right) \right] \\
 & (8-b)
 \end{aligned}$$

$$\begin{aligned}
 & - \frac{1}{R} \frac{\nu Eh}{1-\nu^2} u_{,x} + \left( \frac{1}{R} \right)^2 \left( \frac{Eh}{1-\nu^2} + Gh \right) v_{,\theta} + \\
 & Gh w_{,xx} - \left( \frac{1}{R} \right)^2 Gh w_{,\theta\theta} - \left( \frac{1}{R} \right)^2 \frac{Eh}{1-\nu^2} w + \\
 & Gh \psi_{x,x} + \frac{Gh}{R} \psi_{\theta,\theta} = \\
 & I_1 \ddot{w} - \mu \left[ I_1 \left( \ddot{w}_{,xx} + \frac{1}{R^2} \ddot{w}_{,\theta\theta} \right) \right] \\
 & (8-c)
 \end{aligned}$$

$$\begin{aligned}
 & - Gh w_{,x} + D \psi_{x,xx} - Gh \psi_x + \frac{1}{2} \left( \frac{1}{R} \right)^2 \frac{(1-\nu)D}{2} \psi_{x,\theta\theta} + \\
 & \frac{1}{R} \left( \nu D + \frac{1}{2} \frac{(1-\nu)D}{2} \right) \psi_{\theta,x\theta} = I_2 \ddot{u} + I_3 \ddot{\psi}_x - \\
 & \mu \left[ I_2 \left( \ddot{u}_{,xx} + \frac{1}{R^2} \ddot{u}_{,\theta\theta} \right) + I_3 \left( \ddot{\psi}_{x,xx} + \frac{1}{R^2} \ddot{\psi}_{x,\theta\theta} \right) \right] \\
 & (8-d)
 \end{aligned}$$

$$\begin{aligned}
 & \frac{Gh}{R} v + \frac{Gh}{R} w_{,\theta} + \frac{1}{R} \left( \nu D + \frac{1}{2} \frac{(1-\nu)D}{2} \right) \psi_{x,x\theta} - \\
 & Gh \psi_{\theta} + \frac{1}{2} \frac{(1-\nu)D}{2} \psi_{\theta,xx} + \left( \frac{1}{R} \right)^2 D \psi_{\theta,\theta\theta} = \\
 & I_2 \ddot{v} + I_3 \ddot{\psi}_y -
 \end{aligned}$$

$$\mu \left[ I_2 \left( \ddot{v}_{,xx} + \frac{1}{R^2} \ddot{v}_{,\theta\theta} \right) + I_3 \left( \ddot{\psi}_{\theta,xx} + \frac{1}{R^2} \ddot{\psi}_{\theta,\theta\theta} \right) \right]$$

(8-e)

It is worth mentioning that the above field equations reduce to the classical Donnell shell theory by setting the nonlocal parameter  $\mu$  equal to zero.

### 3. Implementation of the Rayleigh-Ritz Technique

One of the most important matters to apply the Rayleigh-Ritz method in an appropriate way is to describe the components of displacement and rotation as suitable analytical functions which have the capability to predict the behavior of the structure with better convergence and higher accuracy. In the literature, many types of the displacement functions have been implemented with various degrees of success. In the present work, to approximate the vibrational mode shapes of the nonlocal shell corresponding to the various boundary conditions, the functions of polynomial series are utilized to represent the components of displacement as

$$u(x, \theta, t) = U(x) \sin(n\theta) \sin(\omega t)$$

(9-a)

$$v(x, \theta, t) = V(x) \cos(n\theta) \sin(\omega t)$$

(9-b)

$$w(x, \theta, t) = W(x) \sin(n\theta) \sin(\omega t)$$

(9-c)

$$\psi_x(x, \theta, t) = \Psi_x(x) \sin(n\theta) \sin(\omega t)$$

(9-d)

$$\psi_\theta(x, \theta, t) = \Psi_\theta(x) \cos(n\theta) \sin(\omega t)$$

(9-e)

where

$$U(x) = \left( \sum_{e=1}^M A_e x^{e-1} \right) (x)^{n_u^0} (L-x)^{n_u^L} = \sum_{e=1}^M A_e U_e$$

(10-a)

$$V(x) = \left( \sum_{e=1}^M B_e x^{e-1} \right) (x)^{n_v^0} (L-x)^{n_v^L} = \sum_{e=1}^M B_e V_e$$

(10-b)

$$W(x) = \left( \sum_{e=1}^M C_e x^{e-1} \right) (x)^{n_w^0} (L-x)^{n_w^L} = \sum_{e=1}^M C_e W_e \quad (10-c)$$

$$\Psi_x(x) = \left( \sum_{e=1}^M D_e x^{e-1} \right) (x)^{n_{\psi_x}^0} (L-x)^{n_{\psi_x}^L} = \sum_{e=1}^M D_e \Psi_{x_e} \quad (10-d)$$

$$\Psi_\theta(x) = \left( \sum_{e=1}^M E_e x^{e-1} \right) (x)^{n_{\psi_\theta}^0} (L-x)^{n_{\psi_\theta}^L} = \sum_{e=1}^M E_e \Psi_{\theta_e} \quad (10-e)$$

The values of  $n_u, n_v, n_w, n_{\psi_x}$  and  $n_{\psi_y}$  corresponding to different boundary conditions are given in Table 1.

The cylindrical shell used in the nonlocal Donnell shell model is assumed to be symmetric about its mid-shell and its material is linear elastic. The total potential energy functional of SWCNT can be expressed as

$$\Pi(u, v, w, \psi_x, \psi_\theta) = \Pi_K(u, v, w, \psi_x, \psi_\theta) + \Pi_M(u, v, w, \psi_x, \psi_\theta) \quad (11)$$

in which

$$\begin{aligned} \Pi_K(u, v, w, \psi_x, \psi_\theta) = & \frac{1}{2} \int_0^T \int_{\Omega} \left( \left[ \frac{Eh}{1-\nu^2} u_{,x} + \frac{1}{R} \frac{\nu Eh}{1-\nu^2} (v_{,\theta} + w) \right] u_{,x} \right. \\ & + \left[ \frac{\nu Eh}{1-\nu^2} u_{,x} + \frac{1}{R} \frac{Eh}{1-\nu^2} (v_{,\theta} + w) \right] \frac{1}{R} (v_{,\theta} + w) + \frac{Eh}{2(1+\nu)} \left( \frac{u_{,\theta}}{R} + v_{,x} \right) \\ & + D \left( \psi_{x,x} + \frac{\nu}{R} \psi_{\theta,\theta} \right) \psi_{x,x} + \frac{D}{R} \left( \nu \psi_{x,x} + \frac{1}{R} \psi_{\theta,\theta} \right) \psi_{\theta,\theta} + \frac{(1-\nu)D}{2} \left( \frac{\psi_{x,\theta}}{R} + \psi_{\theta,x} \right)^2 \\ & + \frac{Eh}{2(1+\nu)} (w_{,x} + \psi_x)^2 \\ & \left. + \frac{Eh}{2(1+\nu)} \left[ -\frac{\nu}{R} + \frac{w_{,\theta}}{R} + \psi_\theta \right]^2 \right) d\Omega dt \quad (12) \end{aligned}$$

and



$$\begin{aligned}
 \Pi_M(u, v, w, \psi_x, \psi_\theta) &= \frac{1}{2} \int_0^T \int_\Omega \left( [I_1(\dot{u})^2 + I_2(\dot{\psi}_x)^2] \right. \\
 &\quad - \mu \left[ I_1 \dot{u} \left( \dot{u}_{,xx} + \frac{1}{R^2} \dot{u}_{,\theta\theta} \right) + I_2 \dot{\psi}_x \left( \dot{\psi}_{x,xx} + \frac{1}{R^2} \dot{\psi}_{x,\theta\theta} \right) \right] + [I_1(\dot{v})^2 + I_2(\dot{\psi}_\theta)^2] \\
 &\quad - \mu \left[ I_1 \dot{v} \left( \dot{v}_{,xx} + \frac{1}{R^2} \dot{v}_{,\theta\theta} \right) + I_2 \dot{\psi}_\theta \left( \dot{\psi}_{\theta,xx} + \frac{1}{R^2} \dot{\psi}_{\theta,\theta\theta} \right) \right] + I_1(\dot{w})^2 \\
 &\quad - \mu I_1 \dot{w} \left( \dot{w}_{,xx} + \frac{1}{R^2} \dot{w}_{,\theta\theta} \right) \\
 &\quad + [I_2(\dot{u})^2 + I_3(\dot{\psi}_x)^2] \left[ I_2 \dot{\psi}_x - \mu I_3 \left( \dot{\psi}_{x,xx} + \frac{1}{R^2} \dot{\psi}_{x,\theta\theta} \right) \right] + [I_2(\dot{v})^2 + I_3(\dot{\psi}_\theta)^2] \\
 &\quad - \mu \left[ I_2 \dot{v} \left( \dot{v}_{,xx} + \frac{1}{R^2} \dot{v}_{,\theta\theta} \right) \right. \\
 &\quad \left. + I_3 \dot{\psi}_\theta \left( \dot{\psi}_{\theta,xx} + \frac{1}{R^2} \dot{\psi}_{\theta,\theta\theta} \right) \right] \Big) d\Omega dt \tag{13}
 \end{aligned}$$

Using the Rayleigh-Ritz technique, we have

$$\frac{\partial \Pi}{\partial A_e} = \frac{\partial \Pi}{\partial B_e} = \frac{\partial \Pi}{\partial C_e} = \frac{\partial \Pi}{\partial D_e} = \frac{\partial \Pi}{\partial E_e} = 0 \tag{14}$$

Equation (14) leads to  $5 \times M$  linear algebraic equations. By solving the resulting eigenvalue problem, the fundamental frequencies of SWCNTs can be obtained and the associated eigenvectors yield the corresponding mode shapes.

#### 4. Numerical Results and Discussion

The successful application of the nonlocal continuum shell model to free vibration analysis of SWCNTs needs strongly the appropriate values of Young's modulus and effective thickness. In the current study, the thickness of nonlocal shell modeled is assumed to be equal to the spacing of graphite ( $h = 0.34 \text{ nm}$ ). Also, the in-plane stiffness ( $Eh$ ) of SWCNTs can be calculated from the variation of the potential energy with the value of applied compressive axial strain that provides the value of Young's modulus.

According to the above procedure, the values of Young's modulus for both armchair and zigzag SWCNTs are obtained which are approximately the same and are equal to  $1170.39 \text{ GPa}$  and  $1169.72 \text{ GPa}$  respectively. Moreover, the value of density used in the nonlocal shell model can be calculated easily as

$$\rho = \frac{\kappa}{V} = \frac{n \times m}{\pi D h L} \tag{15}$$

where  $\aleph$  is the mass of the nanotube which is equal to  $n$  atoms with the mass of  $m$ .  $V$ ,  $D$  and  $L$  are the volume, diameter and length of the nanotube, respectively. In addition, the Poisson's ratio  $\nu = 0.3$  is considered in the analysis.

Determination of the proper value of nonlocal parameter used in the nonlocal continuum models is an important matter in predicting the response of nanotubes under various load conditions using nonlocal elasticity. The efficiency of the nonlocal continuum shell model developed in section 3 is quite dependent on the recognition of the appropriate value of nonlocal parameter for it.

In the current study, through a nonlinear least square fitting procedure, the appropriate values of nonlocal parameter are derived corresponding to different boundary conditions, as the fundamental frequencies obtained from the two numerical methods namely as MD simulation and Rayleigh-Ritz technique are matched together in which the value of nonlocal parameter is set as the optimization variable. The MD results are taken from [33]. The consistent values of  $\mu$  are given in Table 2 for various boundary conditions and chiralities. It is found that chirality does not have an important role on the proper values of nonlocal parameter. However, the boundary conditions make a significant influence on the values of  $\mu$  proposed from the fitting procedure of the results.

Figures 2-5 illustrate the comparison between the fundamental frequencies obtained from MD simulation and those of nonlocal continuum shell model related to different boundary conditions. The value of nonlocal parameter is changed from zero (local model) to the proper ones obtained through fitting procedure. It can be observed that there is an excellent agreement between the results of developed nonlocal continuum shell model with its proposed proper values of nonlocal parameter and those of MD simulations. Furthermore, it is clearly seen that the local shell model ( $\mu = 0$ ) tends to overestimate the frequencies of SWCNT, especially when its aspect ratio decreases. As the aspect ratio increases, resonant frequencies tend to decrease and the effect of small length scale diminishes so that the frequency envelopes tend to converge. This observation means that the classical continuum model would give a reasonable prediction in the study of nanotubes of high aspect ratios for which the whole structure can be homogenized into a continuum.

## 5. Conclusion

In this work, the vibrational behavior of SWCNTs was studied on the basis of nonlocal continuum elasticity. The Donnell shell theory was employed with Eringen's nonlocal

elasticity equations for considering small scale effects. The Rayleigh-Ritz technique was also used to solve the problem corresponding to four commonly used boundary conditions. The fundamental frequencies of SWCNTs with various aspect ratios and nonlocal parameters were calculated.

To obtain the proper values of nonlocal parameter, MD simulations results were employed. It was found that in contrast to the chirality, the boundary conditions have a considerable influence on the appropriate values of nonlocal parameter. Also, it was observed that the present nonlocal continuum shell model with its proposed consistent values of nonlocal parameter has an excellent capability to predict the vibrational response of SWCNTs which is comparable to the results of MD simulation.

## References

- [1] S. Iijima, *Nature* 354 (1991) 56-58.
- [2] D.H. Kim, C.D. Kim, H.R. Lee, *Carbon* 42 (2004) 1807-1812.
- [3] W.S. Lin, W.J. Liou, C.H. Chen, H.M. Lin, Y.K. Hwu, *Diamond and Related Materials* 18 (2009) 328-331.
- [4] K. Chu, Q. Wu, C. Jia, X. Liang, J. Nie, W. Tian, G. Gai, H. Guo, *Composites Science and Technology* 70 (2010) 298-304.
- [5] R. Smajda, Z. Gyori, A. Sapi, M. Veres, A. Oszko, J. Kis-Csitari, A. Kukovecz, Z. Konya, I. Kiricsi, *Journal of Molecular Structures* 834-836 (2007) 471-476.
- [6] N.G. Sahoo, S. Rana, J.W. Cho, L. Li, S.H. Chan, *Progress in Polymer Science* 35 (2010) pp. 837-867.
- [7] W.X. Chen, J.P. Tu, L.Y. Wang, H.Y. Gan, Z.D. Xu, X.B. Zhang, *Carbon* 41 (2003) 215-222.
- [8] J. Peddieson, G.R. Buchanan, R.P. McNitt, *International Journal of Engineering Science* 41 (2003) 305-312.
- [9] A. Ghorbanpour-Arani, M. Sh. Zarei, *J. Nanostruct.* 5 (2015) 33-40.
- [10] Y.G. Hu, K.M. Liew, Q. Wang, X.Q. He, B.I. Yakobson, *Journal of the Mechanics and Physics of Solids* 56 (2008) 3475-3485.
- [11] Niknam H., Aghdam M.M., *Compos. Struct.*, 119 (2015) 452-462.
- [12] Adhikari S., Gilchrist D., Murmu T., McCarthy M.A., *Mech. Sys. Signal Process.* 60-61 (2015) 583-603.
- [13] R. Ansari, R. Rajabiehfard, B. Arash, *Computational Materials Science* 49 (2010) 831-838.

- [14] Ö. Civalek, C. Demir, *Applied Mathematics and Computation* 289 (2016) 335–352.
- [15] R. Nazemnezhad, M. Zare, *European Journal of Mechanics - A/Solids* 55 (2016) 234–242.
- [16] K. Kiani, 2010, *International Journal of Mechanical Sciences* 52 (2010) 1343-1356.
- [17] H.S. Shen C.L. Zhang, *Composite Structures* 92 (2010) 1073-1084.
- [18] M.J. Hao, X.M. Guo, Q. Wang, *European Journal of Mechanics – A/Solids*, 29 (2010) 49-55.
- [19] M. Nazemizadeh, F. Bakhtiari-Nejad, *Composite Structures* 132 (2015) 772–783.
- [20] K. Amara, A. Tounsi, I. Mechab, E.A. Adda-Bedia, *Applied Mathematical Modelling* 34 (2010) 3933-3942.
- [21] Ö. Civalek, B. Akgöz, *Scientia Iranica* 17 (2010) 367-375.
- [22] J. Yang, L.L. Ke, S. Kitipornchai, *Physica E* 42 (2010) 1727-1735.
- [23] M. Zamani Nejad, A. Hadi, *International Journal of Engineering Science* 105 (2016) 1–11.
- [24] Y. Yan, W.Q. Wang, L.X Zhang, *Applied Mathematical Modelling* 34 (2010) 3422-3429.
- [25] M. Gürses, B. Akgöz, Ö. Civalek, *Applied Mathematics and Computation* 219 (2012) 3226–3240.
- [26] D. Zhou, *International Journal of Solids and Structures* 38 (2001) 5565-5580.
- [27] A. Al-Obeid J.E. Cooper, *Composites Science and Technology* 53 (1995) 289-299.
- [28] O.L. Roufaeil D.J. Dawe, *Journal of Sound and Vibration* 85 (1982) 263-275.
- [29] H.L. Lee, S.S. Chu, W.J. Chang, *Current Applied Physics* 10 (2010) 570-573.
- [30] A.C. Eringen, *International Journal of Engineering Science* 10 (1972) 425-435.
- [31] A.C. Eringen, *Journal of Applied Physics* 54 (1983) 4703-4710.
- [32] L.H. Donnell, 1976, *Beam, Plates and Shells*, McGraw-Hill, New York, USA.
- [33] R. Ansari, H. Rouhi, *Journal of Engineering Materials and Technology* 134 (2012) 011008.

**List of the Tables:**

Table 1: Values of  $n_u$ ,  $n_v$ ,  $n_w$ ,  $n_{\psi_x}$  and  $n_{\psi_y}$  for different boundary conditions

Table 2: Consistent values of nonlocal parameter corresponding to different boundary conditions and chirality

Table 1: Values of  $n_u$ ,  $n_v$ ,  $n_w$ ,  $n_{\psi_x}$  and  $n_{\psi_y}$  for different boundary conditions

| Boundary Conditions  | $n_u$ | $n_v$ | $n_w$ | $n_{\psi_x}$ | $n_{\psi_y}$ |
|----------------------|-------|-------|-------|--------------|--------------|
| Simply supported end | 0     | 1     | 1     | 0            | 1            |
| Clamped end          | 1     | 1     | 2     | 1            | 1            |
| Free end             | 0     | 0     | 0     | 0            | 0            |

Table 2: Consistent values of nonlocal parameter corresponding to different boundary conditions and chirality

| (8,8) armchair SWCNT              |      |
|-----------------------------------|------|
| Simply supported-Simply supported | 0.88 |
| Clamped-Clamped                   | 0.59 |
| Clamped-Simply supported          | 0.56 |
| Clamped-Free                      | 0.86 |
| (14,0) zigzag SWCNT               |      |
| Simply supported-Simply supported | 0.88 |
| Clamped-Clamped                   | 0.59 |
| Clamped-Simply supported          | 0.56 |
| Clamped-Free                      | 0.86 |

**List of the Figures:**

Figure 1: Representation of SWCNTs as cylindrical shell with its coordinate system

Figure 2: comparison of the fundamental frequencies obtained by local and nonlocal models with those of MD simulations corresponding to simply supported-simply supported boundary conditions

Figure 3: comparison of the fundamental frequencies obtained by local and nonlocal models with those of MD simulations corresponding to clamped-clamped boundary conditions

Figure 4: comparison of the fundamental frequencies obtained by local and nonlocal models with those of MD simulations corresponding to clamped-simply supported boundary conditions

Figure 5: comparison of the fundamental frequencies obtained by local and nonlocal models with those of MD simulations corresponding to clamped-free boundary conditions

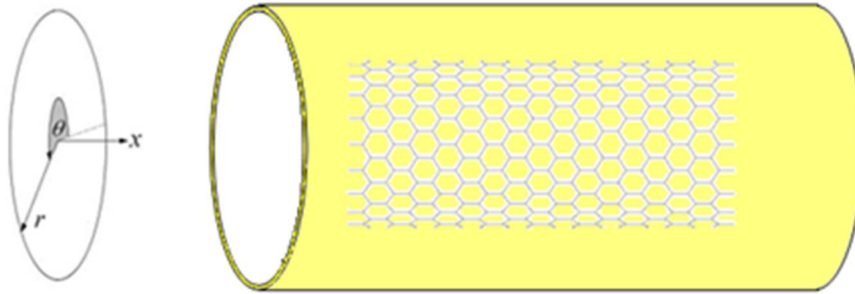


Figure 1: Representation of SWCNTs as cylindrical shell with its coordinate system

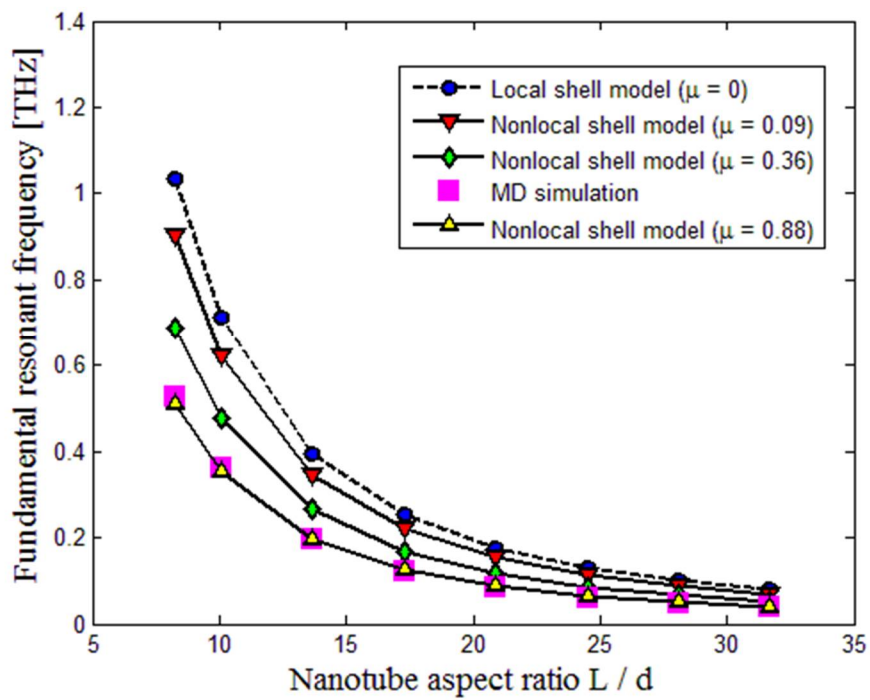


Figure 2: comparison of the fundamental frequencies obtained by local and nonlocal models with those of MD simulations corresponding to simply supported-simply supported boundary conditions

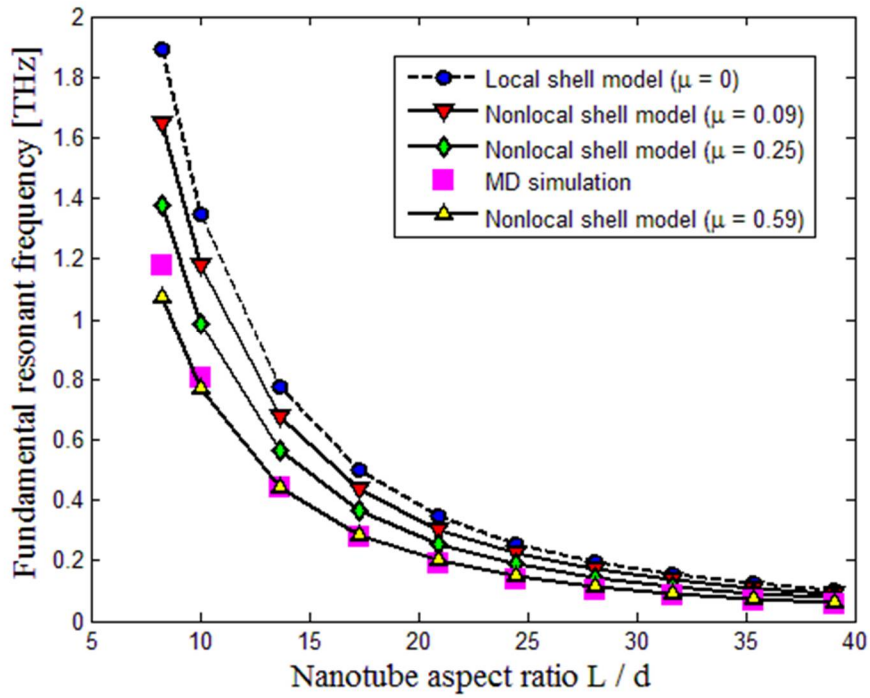


Figure 3: comparison of the fundamental frequencies obtained by local and nonlocal models with those of MD simulations corresponding to clamped-clamped boundary conditions

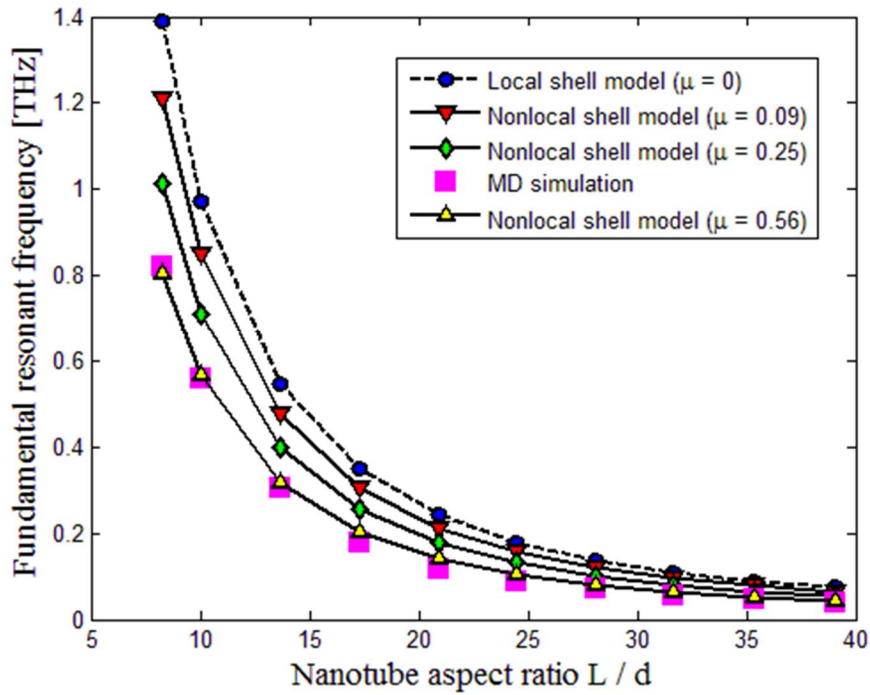


Figure 4: comparison of the fundamental frequencies obtained by local and nonlocal models with those of MD simulations corresponding to clamped-simply supported boundary conditions



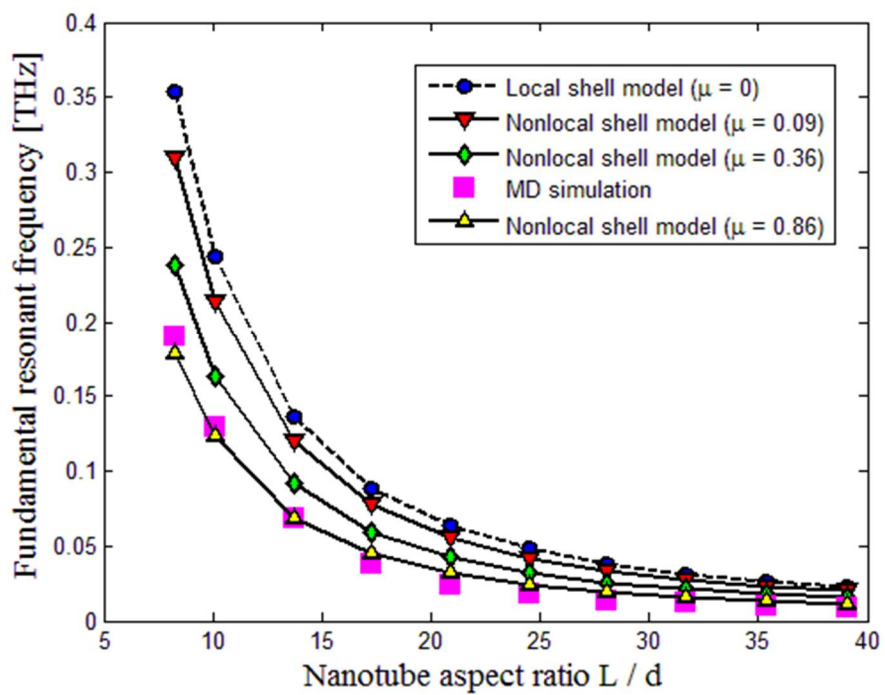


Figure 5: comparison of the fundamental frequencies obtained by local and nonlocal models with those of MD simulations corresponding to clamped-free boundary conditions